JOURNAL OF MATERIALS SCIENCE 12 (1977) 699–707

Transmission electron microscopy observations of misfit dislocations in GaAsP epitaxial films

J. S. AHEARN, C. LAIRD
Department of Metallurgy and Materials Science, University of Pennsylvania, Philadelphia, Pennsylvania, USA

Transmission electron microscopy observations have been made of misfit dislocation structures in GaAsP epitaxial films in foils both parallel to (1) the interface between the epitaxial film and the substrate and (2) the {1 1 1} glide planes. These observations support a near surface source mechanism of dislocation multiplication for relief of the epilayer misfit. It is also suggested that the recently observed surface reconstruction in the III–V compounds might allow for an easier nucleation of dislocations at the surface than hitherto thought. Furthermore, an efficient Lomer dislocation has been observed forming from two 60° glide dislocations thus supporting the hypothesis that all dislocations found in these foils, including the sessile Lomer type, originate from a glide process.

1. Introduction

Two important problems in the introduction of misfit dislocation arrays in epitaxial films of the III–V semiconductors are, first, the source of the 60° glissile misfit dislocations and, second, the origin of the sessile Lomer type dislocations. Both types are found in combination at the substrate–epilayer interface. From the original work of Abrahams *et al.* [1] came the suggestion that threading dislocations bend into the misfit plane during film growth to form a misfit dislocation and, in addition, that the points of junction of coalescing islands of epitaxial film act as sources of dislocations.

Later, Mathews *et al.* [2] proposed that the substrate dislocations act as sources [3, 4] for misfit dislocations in these films through a glide process. Subsequently, Mathews *et al.* [5] have presented evidence that misfit dislocation arrays form through the multiplication of dislocations via the formation and subsequent operation of surface Frank–Read sources. Other results obtained by using stress induced birefringence [6] (SIB) and X-ray toprography [7] (XRT) have supported the suggestion [2, 5] that the surface may act as the primary source of dislocations in these films. There is, therefore, a variety of possible source mechanisms which might operate in these materials.

TEM observations presented here suggest that the surface, along with threading dislocations, are the prime sources of misfit dislocations, which are subsequently multiplied from Frank–Read sources near the surface. In addition, the efficient Lomer dislocations are formed through the interaction of two 60°-glide dislocations in the GaAsP epitaxial system. Two types of TEM samples were prepared: (1) the standard foil thinned parallel to the misfit interface, and (2) a foil thinned parallel to one of the {1 1 1} glide planes passing through the interface at an oblique angle. The oblique section has proved most useful in evaluating the dislocation structure as a function of distance from the misfit interface and in combination with the parallel section has lead to several insights into the process of misfit strain relaxation through the introduction of dislocations.

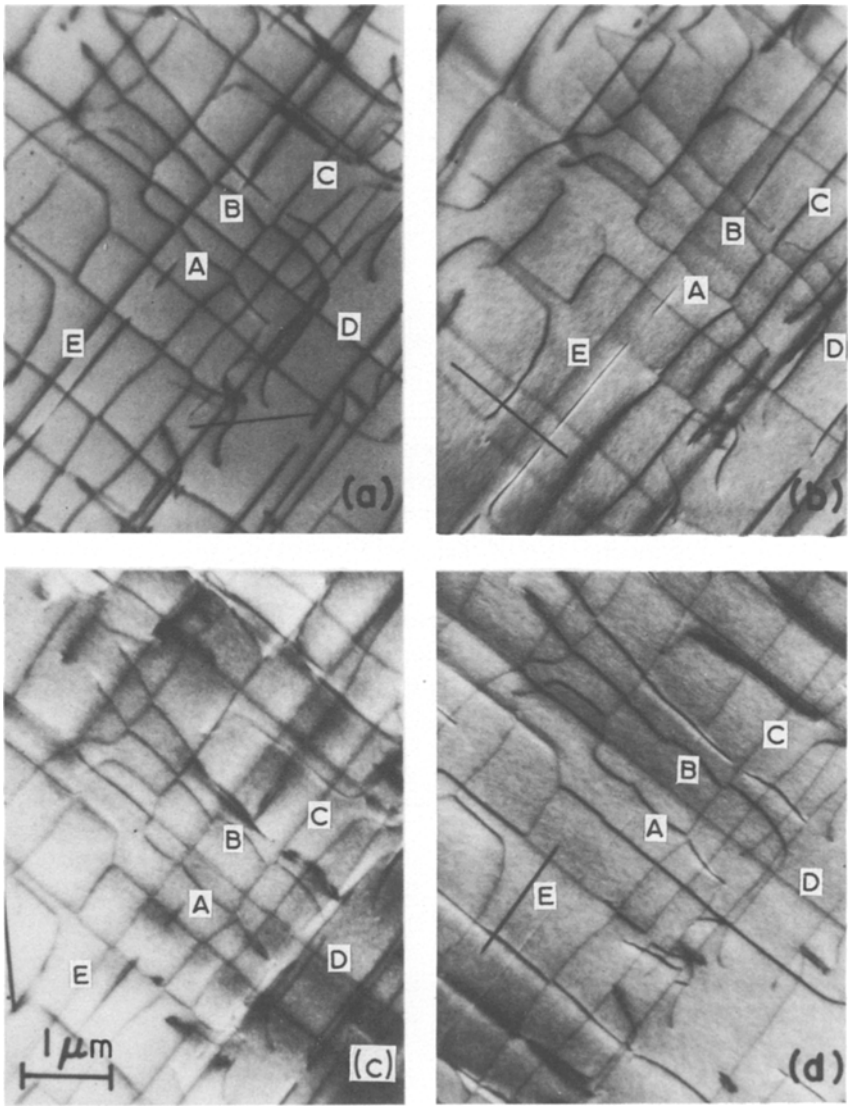

Figure 1 Dislocation structures typical of foils prepared parallel to the near (0 0 1) misfit interface viewed under various reflections: (a) (0 4 0); (b) (2 $\bar{2}$ 0); (c) (4 0 0); (d) (2 2 0).

2. Specimen preparation

Foils for examination by TEM have been prepared by sectioning GaAsP heterojunctions* both parallel to this misfit interface, near (0 0 1), and parallel to {1 1 1} planes believed to be the glide planes of the dislocations which compensate the misfit. The latter section provides a view of the defect structures as a function of distance from the substrate–transition layer interface.

Briefly, foils parallel to (0 0 1) are prepared as follows. Discs of diameter equal to that of the TEM holder are spark-machined from the sheet crystal and are then thinned by mechanical and chemical methods both from the substrate side and epitaxial film side. Thinning is carefully controlled so that the misfit interface is located at the midplane of the disc. At this stage the specimen is 100 μm thick. It is further thinned for

*The $GaAs_{0.49}P_{0.51}$/GaAs and $GaAs_{0.14}P_{0.86}$/GaP samples were purchased from the Monsanto Company, St. Louis, Mo and consisted of either a GaAs or GaP substrate (about 400 μm thick), a transition layer varying from the composition of the substrate to the composition of the final epitaxial layer (about 20 μm thick) followed by the final constant composition layer (about 50 μm thick).

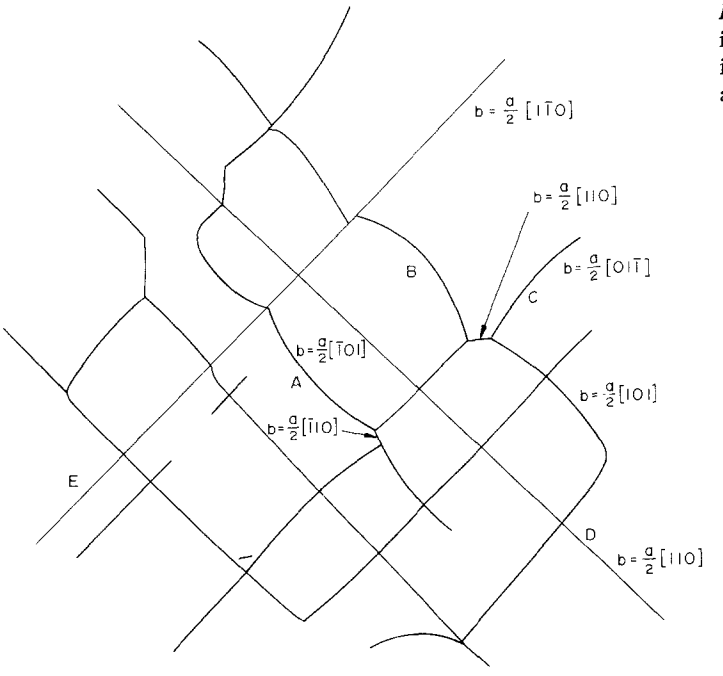

Figure 2 Schematic illustration of the interactions between crossing dislocations including the details of the Burgers vector assignments.

TEM by means of an ion milling apparatus. Attempts to control the region from which the foil is taken have been unsuccessful because the ion milling process is too unpredictable. We, therefore, prepared a large number of specimens so we could obtain a sampling of all the structures present in the films.

In view of this difficulty, the sections cut parallel to the {1 1 1} planes which pass through the misfit interface at an oblique angle have proved to be extremely valuable in characterizing the defect structures as a function of distance from the interface. These samples are prepared by first cutting slices from the sheet crystals oriented with faces parallel to {1 1 1} planes. Two of these samples are then stuck together with epoxy cement so that the epitaxial films from the two samples are in contact except for the thin layer of epoxy. This technique, shown to us by Vermaak [8], effectively increases the width of the sample to twice the thickness of the sheet crystal (about 1 mm) and, in addition, protects the thin epitaxial layer during sample preparation. The composite sample is then thinned by the usual mechanical–chemical methods to about 100 μm. It is finally glued between 3 mm slot-type TEM grids (again using epoxy cement) mounted in the ion milling apparatus and thinned until a hole appears at the appropriate area of the sample. It is possible to determine whether the hole is in the desired location by observing the thin samples in transmitted light. The misfit boundary is clearly apparent from the difference in transmission of the layers having differing compositions. No artefacts attributable to ion-thinning have been observed, and the specimen can be transferred to the microscope with low risk of sample breakage or loss.

3. Results

3.1. Dislocation structures in foils parallel to the epilayer

The dislocation arrays observed in this type of foil have been studied in detail by Abrahams *et al.* [1], Mader and Blakeslee [9] and others. Since the present observations are similar in some respects, a detailed description will not be given and only observations relevant to the discussion below will be presented here. Typical dislocation structures observed in (0 0 1) foils at the same area using two beam conditions and different diffraction vectors are shown in Fig. 1. These arrays normally consist of a square grid of dislocations with the sides of the grid lying along ⟨1 1 0⟩ directions. The dislocations of the grid are generally long and uniform in distribution. Very often, at the intersection of the dislocations, interactions occur which either annihilate a section of dislocation or form a dislocation segment having a different Brugers vector than either of the two

interacting dislocations. By analysing these micrographs we obtained the fraction of dislocations which had Burgers vectors in the misfit interface and which were, therefore, efficient in relieving the misfit strain. This type of dislocation made up 20% of the total number of dislocations observed. The other 80% of the dislocations were of the inefficient type having Burgers vectors at a 45° angle to the misfit plane (in these observations, we agree closely with Mader *et al.* [8]).

Fig. 2 assigns probable Burgers vectors to the bowing dislocation segments of Fig. 1. Dislocations A and B bow out in opposite directions and form segments of dislocation which are oriented differently when they interact with dislocation C. These observations are consistent with A and B lying on glide planes $(\bar{1}\,\bar{1}\,1)$ and $(1\,1\,1)$ respectively and having been introduced into the interface by a glide process; the nucleation site is suspected to be the epilayer surface. Another feature of this figure is the long straight dislocations, D and E, having Burgers vectors in the misfit plane. These dislocations are extremely straight when compared to A and B. An expla-

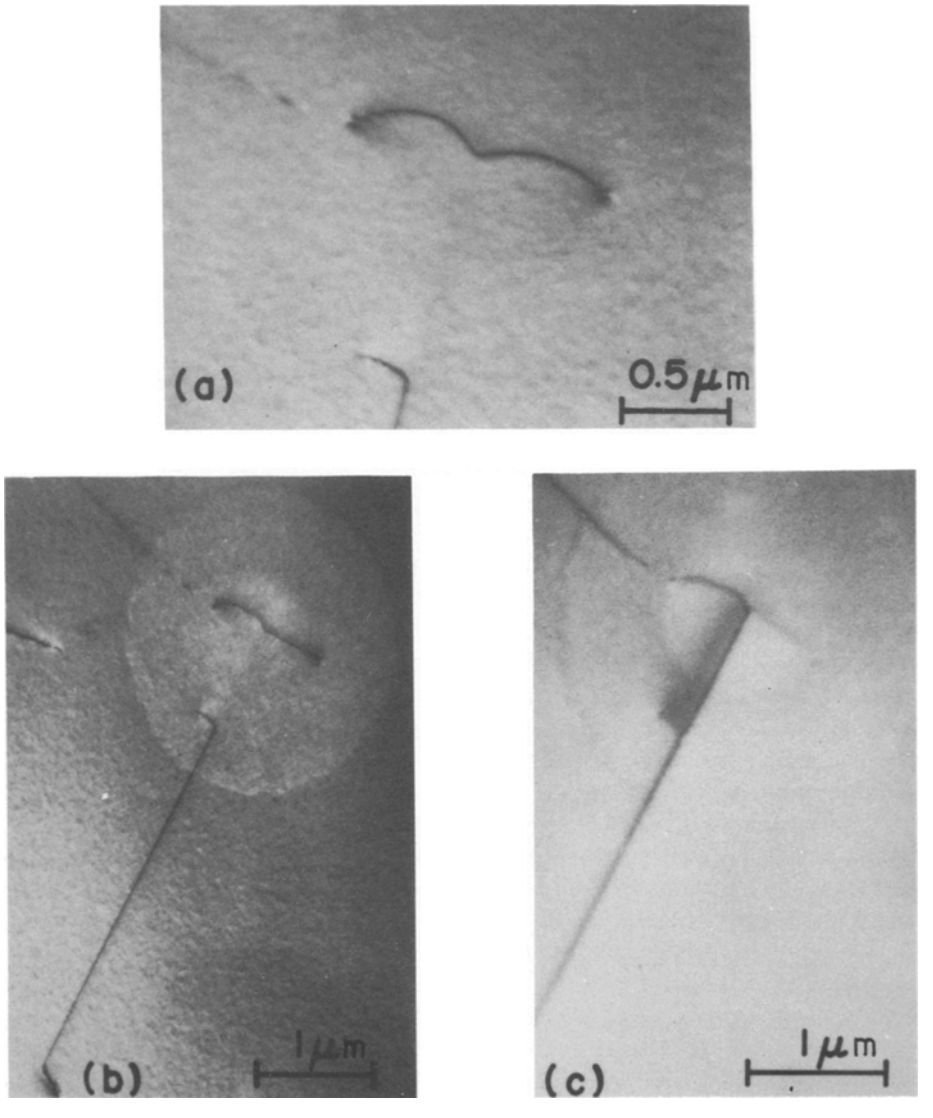

Figure 3 A dislocation reaction showing how efficiently compensating (Lomer) dislocations can be formed: (a) $2\bar{2}\,0$; (b) $2\,\bar{2}\,0$; (c) $4\,0\,0$; (a) was made originally; between (a) and (b) the bowed segments collapsed probably by climb. Note the circle of light material created by the electron beam.

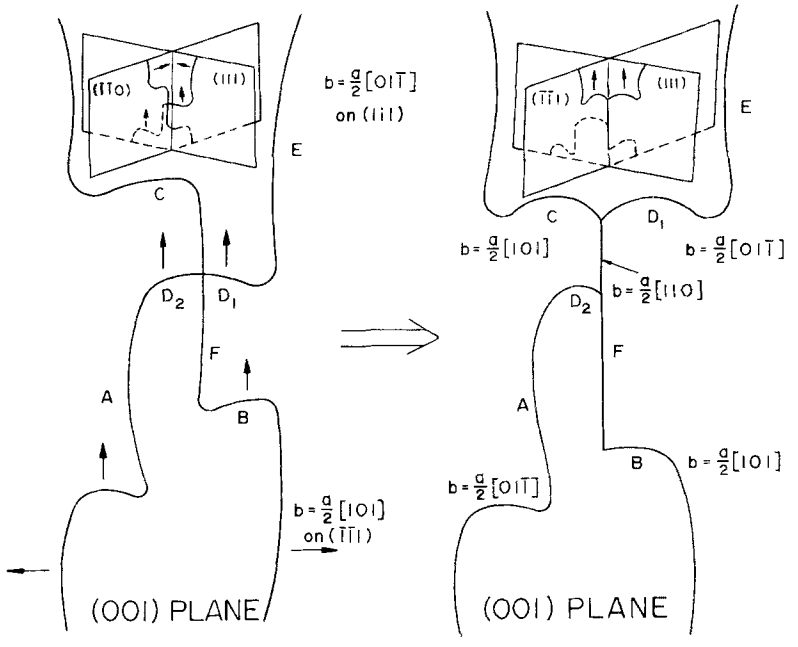

Figure 4 Schematic representation of the reaction shown in Fig. 3.

nation for this observation previously pointed out [10] is that D and E have resulted from an interaction of inefficient dislocations. Consequently, they are of the Lomer type (confined to the intersection of two {1 1 1} planes) and have Burger's vectors of either $\pm 1/2\,a$ [1 1 0] or $\pm 1/2\,a$ [1 $\bar{1}$ 0].

A configuration observed in a GaAsP/GaP sample, reproduced in Fig. 3, illustrates the way in which the efficient dislocations no doubt form. A drawing of this configuration is shown in Fig. 4 with the probable assignment of Burger's vectors. Dislocations AD_2D_1E and BFC lying on the (1 1 1) and ($\bar{1}$ $\bar{1}$ 1) planes respectively come together along the intersections of the glide planes, a (1 1 0) direction. The segment D_1 of AD_2D_1E glides forward to form the efficient dislocation with the resultant formation of the configuration of Fig. 4b. The observed grouping of dislocations in the micrograph is then the segments C, D_1, D_2, F and B, with the efficient dislocation formed between D_1 and D_2. Further glide of segments C and D_1 on the ($\bar{1}$ $\bar{1}$ 1) and (1 1 1) planes creates an efficient dislocation parallel to the misfit interface.

The three-dimensional nature of the dislocation arrays is illustrated in Fig. 5. This micrograph is from a region of the foil which was much thicker than usual. It shows a loose grouping of dislocations along with the apparent blocking of glide dislocations by a Lomer type dislocation (long

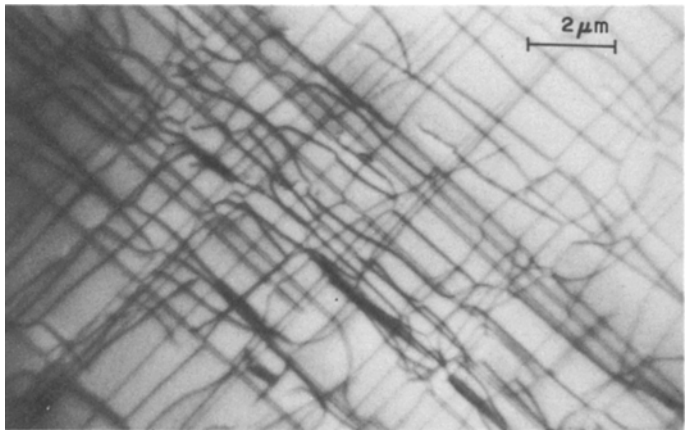

Figure 5 Dislocation arrays typically observed in thicker regions of the samples showing their three-dimensional nature and a loose formation into groups (4 0 0) reflection.

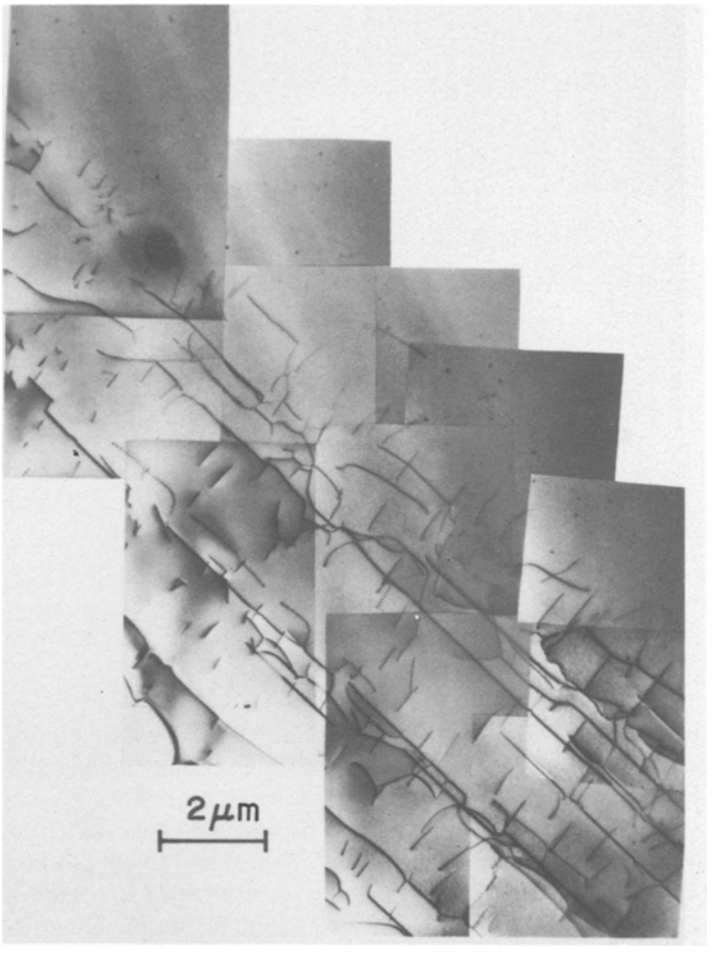

Figure 6 Dislocation array in a foil prepared parallel to a (1 1 1) plane, oblique to the misfit interface. The long dislocations lie approximately in the [1 $\bar{1}$ 0] direction.

straight dislocation exhibiting a double image). The formation of Lomer dislocations in the early stages of the introduction of misfit dislocations and the subsequent behaviour of these dislocations as barriers to the further introduction of dislocations seems to be a significant feature of the strain relaxation process.

3.2. Dislocation structures in foils prepared parallel to a (1 1 1) plane and passing through the misfit interface at an oblique angle

Foils prepared parallel to the (1 1 1) planes have been made from the GaAsP/GaAs system. An example of the dislocation arrays observed in such a foil is shown in Fig. 6. The dislocations extend fairly long distances parallel to the interface and occur in groups. These long dislocations lie approximately in the [1 $\bar{1}$ 0] direction. It is ambiguous, however, whether they are contained in the (1 1 1) foil plane or the ($\bar{1}\,\bar{1}$ 1) glide plane intersecting the (1 1 1) plane along [1 $\bar{1}$ 0].

The groups of dislocations are separated by approximately 2.0 to 2.5 μm in the (1 1 1) plane. Regions between the groups are free of dislocations lying on (1 1 1) or ($\bar{1}\,\bar{1}$ 1) but do contain dislocations which lie on either ($\bar{1}$ 1 $\bar{1}$) or (1 $\bar{1}\,\bar{1}$). There are again two types of dislocations: the efficient type which appear as very straight dislocations lying quite accurately in the [1 $\bar{1}$ 0] direction, and inefficient dislocations which are curved and deviate often significantly from the [1 $\bar{1}$ 0] direction.

A further significant observation is the large number of dislocation interactions and the interconnection of the dislocations into a network both by dislocations which lie on the (1 1 1) planes and by the dislocations lying on the other glide planes which appear only as relatively short dislocation segments. From Fig. 6 it is apparent that dislo-

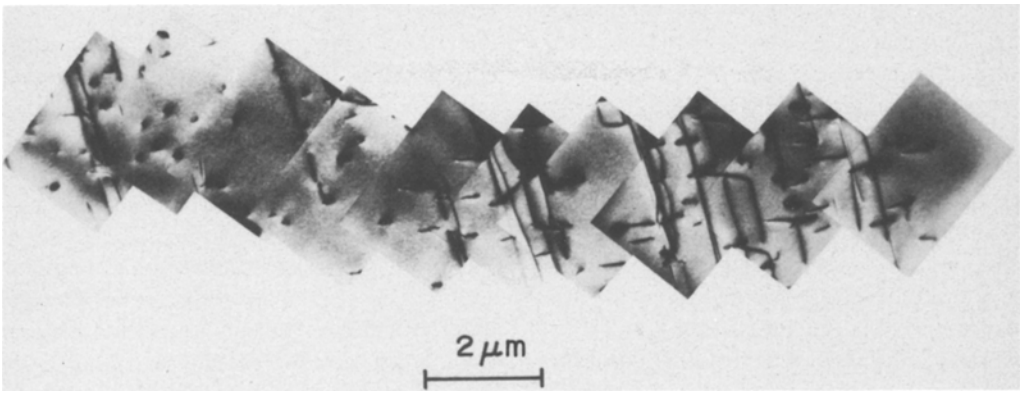

Figure 7 Oblique section illustrating the extent of the dislocations from the substrate.

cation interactions are extremely important in the introduction of dislocations into the misfit interface. The formation of the dislocation arrays prevents the further movement of dislocations into the interface because of the large number of interactions which do occur.

An additional interesting feature of the oblique sections is the sharp discontinuity between the regions containing dislocations and the regions which do not contain dislocations.

In addition to the observation of dislocations arrays, singular spots can also be seen in Fig. 6. The precise nature of these spots is difficult to determine. We speculate that they are either very small dislocations loops or precipitates formed from a dopant upon cooling from the growth temperature. The "spot" pattern occurs mainly in the epitaxial layer away from the region where the dislocations form.

A second mosaic of an oblique section is shown in Fig. 7 where we illustrate the extent of the dislocation arrays starting at the substrate and proceeding into the epitaxial films. This section covers more than 18 μm on the (1 1 1) plane corresponding to a distance of 10 μm in a direction normal to the interface. This distance is approximately half way through the transition region of the epitaxial film. The absence of the spot pattern in the substrate is of interest. If this pattern occurs only in the epitaxial layer, which seems to be the case, then the source of this pattern apparently is connected with film growth. This could mean that an excess of point defects develops as the epitaxial deposition takes place. The point defects subsequently condense into the spots on cooling in the absence of dislocations but may adsorb onto the dislocations in the regions where the dislocation densities are high.

4. Discussion

By application of the XRT and SIB methods, other work [6, 7] has demonstrated the importance of the geometrical relationship between the glide planes and the misfit interface for the final arrangement of misfit dislocations. The apparent lack of similar observations using TEM reported here seems to be inconsistent with those results. However, the TEM observations are generally made at high magnification where such differences are difficult to observe. In addition, the dislocations can appear locally parallel to the ⟨1 1 0⟩ directions but have a net 3° deviation from this direction over large distances (hundreds of microns).

It was also concluded [6, 7] that the dislocations originated initially from surface sources or threading dislocations and that these immediately interacted to form predominant Frank–Read sources, that they occur in groups and that the dislocation groups lie parallel to the misfit interface over long distances (mm). The present study of oblique TEM sections has confirmed the grouping of dislocations on the {1 1 1} glide planes further supporting the mechanism of glide dislocation sources.

The observations of dislocation arrays in foils parallel to the interface are similar to those made previously by others. The analysis of the arrays given here reinforces the conclusion [2, 10] that the majority of dislocations are introduced by glide on {1 1 1} planes during film growth. The large number of dislocation interactions found in

the arrays in both the oblique and parallel foils suggests the importance of work hardening during the misfit dislocation formation. The new information presented here of the formation of an efficient misfit dislocation supports the suggestion that the efficient dislocations form from 60° glide dislocations by dislocation interactions.

In addition, our observations coupled with those of previous studies suggest the following sequence of events for the formation of the dislocation arrays. During the initial film growth, substrate dislocations act as threading dislocation sources of misfit dislocations when the critical thickness required for their glide is reached. Once this process terminates, as it must do quite soon because of the low density of the substrate dislocations, dislocations are activated from surface sources and glide into the interface on {1 1 1} glide planes. The observations in oblique sections indicates that a small number of dislocations (about 5) are generated from each source at a given time and glide large distances away from the source location. In the process of this glide, the dislocations interact and form near-surface Frank–Read Sources. There is perhaps then a waiting period until the strain builds during film growth to a critical value for further source operation. At this point the sources are activated on the same or a closely adjacent glide plane and the process repeats itself. The source operation is probably halted by a combination of (1) the work hardening process resulting from the activation of other intersecting glide planes with the subsequent formation of Lomer dislocations and the performance of these sessile dislocations as barriers to further motion, and (2) by the decrease in driving force for dislocation motion caused by a decrease in misfit resulting from the introduction of the initial dislocations. The threading dislocations present in the epilayer probably result from dislocations which were unable to glide further due to dislocation interactions and a decrease in the driving force acting on the dislocations once the thickness of the graded layer was obtained. These dislocations become immobile and simply grow into the epilayer approximately normal to the film surface. Similar suggestions as to the source of threading dislocations have already been made for a GaP/GaP system [11].

It seems most likely that the major sources of dislocations in these films are surface or near surface sources leading to the creation of further near-surface Frank–Read sources by dislocation interaction. The major evidence supporting this conclusion is the very long dislocation lines observed by TEM, SIB [6] and XRT [7] methods combined with the present TEM observations indicating that the arrays of long parallel dislocations occur in distinct groups throughout the transition layer (about 20 μm). To explain these observations, it seems necessary to have fresh sources activated at the epilayer surface as film growth proceeds. These newly generated dislocations would then have a free, almost unhindered, glide path away from the source location and should be able to glide throughout the film.

Theoretical estimates [12, 5] have been made of the stress needed for nucleation of a dislocation half-loop at a stepped surface. Although these estimates have never been experimentally verified it is generally believed that surface nucleation does not occur at reasonably low stress levels. Indeed we would not expect such activation in the films of interest here from these estimates. However, the recent results showing surface reconstruction [13] of GaAs and the postulated existence of dislocations at reconstructed steps in these materials [14] indicate that the surface can indeed act as a ready source of dislocations.

Acknowledgements

Valuable discussion with Dr C. A. B. Ball about interpretation and useful suggestions from Mr R. White about handling and preparing the TEM specimens are gratefully acknowledged, as in the financial support of the Office of Naval Research under Grants No. N00014-A-0121-0031 and N00014-76-C-0360.

References

1. M. S. ABRAHAMS, L. R. WEISBERG, C. J. BUIOCCHI and J. BLANC, *J. Mater. Sci.* **4** (1969) 223.
2. J. W. MATHEWS, S. MADER and T. B. LIGHT, *J. Appl. Phys.* **41** (1970) 3800.
3. J. W. MATHEWS, *Phil. Mag.* **13** (1966) 1207.
4. W. A. JESSER and J. W. MATHEWS, *ibid* **15** (1967) 1097.
5. J. W. MATHEWS, A. E. BLAKESLEE and S. MADER, *Thin Solid Films* **33** (1976) 253.
6. J. S. AHEARN, C. A. B. BALL and C. LAIRD, *Phys. Stat. Sol.* **38** (1976) in press.
7. J. S. AHEARN and C. LAIRD, *Bull. Amer. Phys. Soc.* **20** (1975) 444; J. S. AHEARN, C. A. B. BALL and C. LAIRD, *Thin Solid Films*, in press.
8. J. H. VERMAAK, private communication, University of Port Elizabeth, Republic of S. Africa.

9. S. MADER and A. E. BLAKESLEE, *IBM J. Res. Div.* **19** (1975) 151.
10. S. MADER, A. E. BLAKESLEE and J. ANGILELLO, *J. Appl. Phys.* **45** (9174) 4730.
11. G. B. STRINGFELLOW, P. F. LINDQUIST, T. R. CASS and R. A. BURMEISTER, *J. Electron Mater.* **3** (1974) 497.
12. J. P. HIRTH, in "Relation Between Structure and Strength in Metals and Alloys" (H. M. S. O., London, 1963) p. 218.
13. F. JONA, *IBM J. Res. Dev.* **9** (1965) 375.
14. D. L. RODE, *Phys. Stat. Sol.* (*a*) **32** (1975) 425.

Received 21 July and accepted 27 July 1976.